Substrate Competitive Inhibitors of IGF-1 Receptor Kinase

Galia Blum,[‡] Aviv Gazit,[‡,§] and Alexander Levitzki*

Department of Biological Chemistry,The Alexander Silberman Institute of Life Sciences, Department of Organic Chemistry, Institute of Chemistry, The Hebrew University of Jerusalem, Givat Ram, Jerusalem 91904, Israel

Received June 30, 2000

ABSTRACT: IGF-1 and its receptor play a pivotal role in many cancers, and therefore, IGF-1R is an attractive target for the design of inhibitors. In this communication, we report on a number of lead compounds for inhibitors of the isolated IGF-1R kinase. The search for these compounds utilized two novel in vitro assays and was aided by the knowledge of the three-dimensional structure of the insulin receptor kinase domain, which is 84% homologous to the IGF-1R kinase domain. The most potent inhibitor found in these assays was tyrphostin AG 538, with an $IC_{50} = 400$ nM. In computer modeling, AG 538 was placed in the kinase domain of the insulin receptor and was able to sit in place of tyrosines 1158 and 1162, which undergo autophosphorylation. Experimentally it is indeed found that AG 538 does not compete with ATP but competes with the IGF-1R substrate. We prepared I-OMe AG 538, which is more hydrophobic and less sensitive to oxidation than AG 538. Both AG 538 and I-OMe AG 538 inhibit IGR-1R autophosphorylation in intact cells in a dose-dependent manner but I-OMe-AG 538 is superior, probably because of its enhanced hydrophobic nature. Both compounds inhibit the activation of the downstream targets PKB and Erk2. These findings suggest that AG 538 and I-OMe-AG 538 can serve as a lead compound for the development of substrate competitive inhibitors of the IGF-1R. The possible advantage of substrate competitive inhibitors vis-à-vis ATP competitive inhibitors is discussed.

INTRODUCTION

The insulin-like growth factor 1 receptor (IGF-1R) and the insulin receptor (IR) are structurally highly related glycoproteins. Both possess two extracellular α-subunits, which bind the ligand, and two β subunits, which span the membrane and possess the intracellular autophosphorylation sites. Upon ligand stimulation, the β subunits undergo autophosphorylation and become catalytically active. In contrast to insulin, which is mostly a metabolic hormone, IGF-1 is involved in normal cell proliferation and has been implicated in oncogenesis (*1*−*4*). The IGF-I ligand, its receptor, the IGF-1 binding proteins, and the specific proteolytic enzymes which degrade these proteins constitute an important regulatory system which plays a pivotal role in normal and neoplastic cell growth (*5*). In many tumors, such as lung cancer (*6*), colon carcinoma (*7*), tumors of the CNS (*8*), cervical cancer (*9*), and Wilms tumor (*10*), IGF-1 signaling is enhanced due to overexpression of its receptor or constitutive autocrine signaling. The key role that the IGF-1R receptor plays in promoting tumorigenesis has been suggested by a number of studies. Expression of dominant negative IGF-1R in IGF1-R-expressing Rat-1 fibroblasts inhibits tumorigenesis (*11*). Blocking the IGF-1R with specific antibody against the receptor inhibits the growth of human breast cancer cells (*10*, *12*) and of Wilms tumor cells in culture and in nude mice (*13*). Expression of antisense RNA directed against the IGF-1R mRNA lowers the expression of the IGF-1R in human breast cancer cells and significantly decreases their growth rate (*14*). In rhabdomyosarcoma (RMS) cells, IGF-1R antisense also inhibits the malignant phenotype (*15*). Overexpression of the wild-type human IGF-1R induces ligand-dependent neoplastic transformation of NIH-3T3 cells and tumor growth in nude mice (*16*). IGF-1R signaling probably plays an important role during carcinogenesis by inhibiting apoptosis (*17*, *18*), and at least some of its anti-apoptotic actions are mediated by c-Akt/PKB (*19*). This activity of the IGF-1R is distinct from its mitogenic activity and presumably is transmitted by different domains of the receptor (*20*). The pivotal role of IGF-1R and its anti-apoptotic activity point to this receptor as a potential target for anti-cancer drugs (*21*).

In 1994, the three-dimensional structure of the tyrosine kinase domain of the human insulin receptor was determined at 2.1 Å resolution (*22*). In the inactive conformation, tyrosine 1162 binds to aspartic acid 1132 and prevents access of the substrate to the catalytic loop. Upon ligand binding, tyrosines 1158, 1161, and 1162 undergo autophosphorylation and swing out, enabling substrate binding (*23*). These tyrosines are essential for the activation of the receptor. Because of the very high degree of homology between the insulin receptor and IGF-1R kinase domains, we decided to take advantage of the known three-dimensional structure of the IR in an attempt to select candidates for IGF-1R kinase inhibitors. Initial screening of tyrphostins had already identified a family of compounds, which block IGF-1R kinase (*24*).

In this communication, we describe our initial success in generating IGF-1R kinase inhibitors and establish two novel in vitro assays that facilitate screening for IGF-1R kinase inhibitors. Structure activity relationships of several com-

* To whom correspondence should be addressed. Phone: 972-2-6585404. Fax: 972-2-6512958. E-mail: levitzki@vms.huji.ac.il.

[‡] The Alexander Silberman Institute of Life Sciences.

[§] Department of Organic Chemistry.

10.1021/bi001516y CCC: $19.00
Published on Web 11/28/2000

pounds that inhibit the IGF-1R autophosphorylation or substrate phosphorylation were determined using these assays. Several potent compounds were identified. These may be useful leads for chemotherapeutic agents.

MATERIALS AND METHODS

Protease inhibitors, phosphatase inhibitor, immobilized lectin beads, *N*-acetyl-D-glucoseamine, bovine serum albumin (BSA), poly(Glu, Tyr) 4:1, IGF-1, and diphosphorylated MAP kinase antibodies (phospho Erk) were from Sigma. A hybridoma producing anti-IGF-1R-α antibodies (16−13) was a generous gift from Prof. Axel Ullrich, from the Max Planck Institute (Martinsreid, Germany). Anti-IGF-1R-α antibodies used for the in vitro autophosphorylation assay were generated by precipitation from the hybridoma medium with ammonium sulfate and further purified on a protein A column. Anti-Akt1, Erk2, anti-IGF-1R β antibodies were from Santa Cruz Biotechnology, and anti-phospho-Akt (Ser 473) antibody was from New England Biolabs. Medium from a hybridoma producing anti-phosphotyrosine 4G10 was used for imunoblotting. DMSO was from BDH. ATP $\gamma[^{32}P]$ was purchased from Amersham Life Science, 3MM paper for radioactive assay was from Whatman Inc. The REGRESSION program was from Blackwell Scientific Software, Osney Mead, Oxford, U.K.

Synthesis of I-OMe AG 538. I-OMe AG 538 was synthesized as was AG 538 (*25*), with slight changes: 0.8 M 2-chloro 3,4-dihydroxyacetophenone was added to 0.085 M KCN in 10% DDW/DMSO. These were stirred at 100 °C for 3 h. A total of 200 mL of DDW and 20 mL of concentrated HCl were added to the reaction mixture and stirred for an additional 30 min. The product was then extracted with 3 × 200 mL of ethyl acetate, and subsequently evaporated, followed by chromatography on silica gel 70-230. 2-Cyano 3,4-dihydroxyacetophenone was eluted with 2% methanol in dichloromethane, with a yield of 11.8%. Reflux of 10 mM 2-cyano 3,4-dihdroxyacetophenone, 10 mM 5-iodovanilline, and 0.1 g of β-alanine was performed for 5 h in ethanol, followed by evaporation and chromatography on silica gel 70-230, elution with 3% methanol in dichloromethane, and recrystallization in hexane/ethanol. Overall yield was 39%. Tyrphostins were prepared as described previously (*26*−*30*).

Cell Culture. NIH-3T3 mouse fibroblast cells overexpressing wild-type IGF-1R at approximately 700 000 receptors/cell (clones NWTc34 and NWTc43) or insulin receptor (clone WTIR) were a generous gift from Dr. D. LeRoith (*2*). Cells were cultured in DMEM supplemented with 10% FCS, 100 units/mL penicillin, 100 μg/mL streptomycin, and 500 μg/mL Geneticin (G418), in a humidified atmosphere of 94% air and 6% CO_2 at 37 °C.

R^+ and R^- cells were a generous gift from Dr. R. Baserga. R^- cells are mouse embryo fibroblasts, which are 3T3-like cells devoid of IGF-IR (*31*). R^+ cells were generated by stable transfection of IGF-1R at approximately 1×10^6 copies to R^- cells (*31*). Cells were cultured in DMEM supplemented with 10% FCS, 100 units/mL penicillin, 100 μg/mL streptomycin, 50 μg/mL G418, and 50 μg/mL hygromycin B, in a humidified atmosphere of 94% air and 6% CO_2 at 37 °C.

Partial Purification of the IGF-1R. Purification of the IGF-1R was performed based on the IR purification method described earlier (*32*). Confluent R^+ cells overexpressing the IGF-1R were lysed in the presence of 10% glycerol, 50 mM HEPES, 1% Triton X-100, 150 mM NaCl, 5 μM EGTA, 0.24 mg/mL AEBSF, 10 μg/mL aprotinin, 5 μg/mL leupeptin, 25 mM benzamidine, and 10 μg/mL soybean trypsin inhibitor. The lysate was bound to immobilized lactin overnight at 4 °C, and washed with HTN buffer (50 mM HEPES, 1% Triton X-100, and 150 mM NaCl). Additional washes were with 50 mM HEPES, 1% Triton X-100, 1 M NaCl, and then with 10% glycerol/HTN. Semi-purified IGF-1R was eluted with 0.5 M *N*-acetyl-D-glucoseamine + 10% glycerol/HTN, frozen and kept at −70 °C.

Inhibition of IGF-1R Autophosphorylation in Cell-Free System. Inhibition of tyrosine autophosphorylation of the purified IGF-1R was analyzed by an ELISA assay. Ninety-six-well polypropylene plates were coated overnight at 4 °C with purified antibodies against the β-subunit of IGF-1R (16-13). Plates were blocked with 5% BSA in PBS and washed, and 100 μg/well of cell lysate from the IGF-1R overexpressors, NWTc34 or NWTc43, was added. The lysates were obtained in the presence of 10% glycerol, 50 mM HEPES, 1% Triton X-100, 150 mM NaCl, 5 μM EGTA, 1 mM PMSF, 10 μg/mL aprotinin, 5 μg/mL leupeptin, 25 mM benzamidine, and 10 μg/mL soybean trypsin inhibitor. The plates were incubated for 30 min and washed. A total of 135 μL of tyrphostins at different concentrations was added in 5% DMSO/TBS for 30 min prior to kinase activation. Tyrosine phosphorylation was achieved by the addition of 15 μL of kinase buffer to yield a final concentration of 30 mM HEPES, 12 mM $Mg(Ac)_2$, 0.04 mM $NaVO_3$, 5 mM $Mn(Ac)_2$, and 15 μM ATP, and the mixture was incubated at 26 °C for 30 min. The reaction was terminated by the addition of 16.5 μL of 200 mM EDTA, pH 8.0. Phosphorylated tyrosines were bound to rabbit polyclonal anti-phosphotyrosine serum (1:3000) for 45 min, followed by anti-rabbit peroxidase conjugate antibody for 30 min. Detection was carried out with a color reagent, 2,2′-azido-bis 3-ethylbenzihiazoline-6-sulfonic acid (ABTS) in citrate-phosphate buffer, pH 4.0, with 0.004% H_2O_2 for 30 min and monitored at O.D 405 nm. IC_{50} values of inhibitors were determined using the REGRESSION program.

Inhibition of IGF-1R-Catalyzed Substrate Phosphorylation. The general PTK substrate poly(Glu, Tyr) 4:1, (pGT), was coated onto a 96-well polypropylene plate (12.5 μg/well). Semipurified IGF-1R from R^+ cells was incubated (10 ng/well) in 20 μM ATP, 10 mM $MgCl_2$, 5mM $MnAc_2$, and 20 mM Tris·HCl, pH 7.4, with or without inhibitors, for 20 min at 30 °C. The plate was washed and blocked with 5% low-fat milk, and pGT phosphorylated tyrosines were measured and detected as above. The assay was optimized with respect to the amount of IGF-1R and phosphorylation conditions. The signal was linear for 30 min and as a function of IGF-1R protein concentrations up to 35 ng/well.

Inhibition of IGF-1R Substrate Phosphorylation by Radioactive Methods. A total of 200 ng/system of semipurified IGF-1R from R^+ cells were added to a solution containing AG 538 and pGT at various concentrations. The reaction was initiated by the addition of reaction buffer [30 mM HEPES, 12 mM $Mg(Cl)_2$, 0.04 mM $NaVO_3$, 5 mM $Mn(Ac)_2$, 125 μM ATP, and 1.5 μCi/system ATP γ $[^{32}P]$, final concentration] at 30 °C for 10 min. The reaction was stopped by the addition of EDTA, pH 8, 0.1 M final concentration.

Reaction samples were absorbed on to 3MM Whatman paper squares. The papers were then washed in 10% TCA, 1% sodium pyrophosphate at room temperature, and dried in ethanol. Radioactivity on the papers was measured by a scintillation counter. The data were analyzed by a computer best-fit curves using a program that was written for this purpose (*33*) and also analyzed by the Microsoft Excel program. IC_{50} values were determined using the REGRESSION program.

Inhibition of Autophosphorylation of IGF-1R in Intact Cells. Tyrosine autophosphorylation of the β-subunit of IGF-1R was assayed as described (*24*) with minor modifications. Briefly, subconfluent NWTc43 cells in 6-well polypropylene plates were incubated for 6 or 15 h with inhibitor at various concentrations in DMEM supplemented with 10% FCS, 100 units/mL penicillin, 100 μg/mL, 0.1% DMSO, and 0.1% ethanol. (The final concentration of DMSO/ethanol was kept constant in all systems.) Cells were then starved for 1 h in DMEM, containing inhibitors at the same concentration as before, in 0.1% DMSO and 0.1% ethanol. Cells were then stimulated with 5 ng/mL IGF-1 for 5 min. After IGF-1 treatment, cells were washed twice with ice-cold PBS and lysed by addition of boiling sample buffer (10% glycerol, 50 mM Tris·HCl, pH 6.8, 3% sodium dodecyl sulfate, and 5% β-mercaptoethanol). Lysates were boiled for 10 min and cleared by centrifugation. Equal amounts of protein per lane were separated by 6% SDS−PAGE and transferred to a nitrocellulose membrane. Phosphorylated proteins were immunoblotted with monoclonal anti-phosphotyrosine, anti-phospho-Akt (Ser 473), and anti-phospho EKR antibodies. Detection was performed with horseradish-peroxidase-conjugated secondary antibody using an ECL system. Blots were then stripped of antibodies by incubating in 2% SDS, 10 mM β-mecaptoethanol, Tris·HCl, pH 6.8, 62.5 mM at 55 °C for 20 min, blocked, and reprobed with anti-IGF-1Rβ, anti-Akt1, and anti-Erk2 antibodies, respectively, and detected as above. Band intensities were quantified using the NIH image program.

Inhibition of IR-Catalyzed Substrate Phosphorylation. Inhibition of substrate phosphorylation of insulin receptor tyrosine kinase (IRK) was performed in the presence of AG 538. IRK assay was identical to IGF-1R substrate phosphorylation assay with three modifications: semipurified (WGA) IR from WTIR cells was used instead of IGF-1R (R^+, WGA), and 13 ng of IR was used per well and reaction time with ATP was 17 min. The signal was linear with phosphorylation time up to 20 min and with IR protein concentration up to 50 ng/well.

Presentation of Molecules. The most effective IGF-1R kinase inhibitor, AG 538, was built, minimized and presented with the Insight II, version 2.2.0, program of the Biosym Technologies package.

RESULTS

Screen for Inhibitors of Tyrosine Autophosphorylation of the IGF-1R. A fast and nonradioactive assay for inhibitors of IGF-1R autophosphorylation was used to screen tyrphostins. The assay was based on binding IGF-1R onto an α-IGF-1R antibody-coated plate to which potential inhibitors and kinase buffer were then added. Phosphotyrosine was detected by a colorimetric assay as described in the Materials and Methods. Activities were measured plus or minus inhibitors and IC_{50} values were calculated, as described in Materials and Methods. Tyrphostins representing different families, synthesized in our laboratory, were analyzed by this ELISA assay as potential IGF-1R autophosphorylation inhibitors. Most of the tyrphostins we chose to screen possessed two aromatic rings, resembling the orientation of the two tyrosines, 1158 and 1162, in the catalytic loop of the IR. Table 1 summarizes the potencies of members of four tyrphostin groups as IGF-1R kinase autophosphorylation inhibitors in this cell-free assay.

A few structural elements of the molecule were found to be important for the potency of these compounds. The addition of iodine to the catechol ring (AG 974 and AG 1049 of group B) improved significantly the potency of compounds with one aromatic ring as compared to the other compounds in the group (Table 1B). Replacement of the oxygen in the carbonyl group of some tyrphostins with sulfur (AG 213 and AG 1007) increased the inhibition markedly (Table 1C). Molecules which possess two catechol groups were found to be highly potent inhibitors (Table 1, parts A and D). Thirteen blockers were found to possess IC_{50} values under 10 μM, all of these contained two aromatic rings. Three of these molecules had IC_{50} values under 1 μM.

Screen for Inhibitors of poly-Glu_4-Tyr (pGT) Phosphorylation by IGF-1R. A second assay, screening for IGF-1R substrate inhibitors, was based on the phosphorylation of pGT. Poly-GT was coated onto a plate, and phosphorylated by the addition of semipurified IGF-1R, with or without inhibitor (see Materials and Methods). Phosphotyrosine was detected as above and IC_{50} values were determined.

In this screen, 120 hydrophobic tyrphostins were chosen for screening. These compounds were chosen since they are likely to penetrate the cell membrane and thus could potentially inhibit the receptor in intact cells. Most of the compounds were not very potent, but three compounds were found to possess IC_{50} values under 10 μM. Table 2 presents structure function relationships of the more potent inhibitors found in this assay.

The structure function analysis showed that both the hydroxyls in the catechol group are essential for inhibitor potency, as exemplified by the comparison of AG 568 to AG 1843 (Table 2B). In order for a compound to exhibit improved inhibitory activity, it must contain a catechol ring. This finding was true for both of the cell free assays.

Comparison of AG 538 with Tyrosine-Autophosphorylation Site of the IR. AG 538 was found to be the most potent inhibitor, blocking autophosphorylation with IC_{50} of 400 ± 200 nM (Table 1C) and blocking substrate phosphorylation with an IC_{50} of 61 ± 20 nM (Table 5) in the presence of 20 μM ATP. We therefore examined if one can "embed" this compound in the IGF-1R kinase domain. In the absence of a known crystal structure for the IGF-1R kinase domain, we used the highly homologous (84% identical) structure of the IR kinase domain (*22*). AG 538 was built and minimized with the Insight program. AG 538 was then superimposed over tyrosines 1158 and 1162 of the insulin receptor structure. The resemblance of the two molecules is presented in Figure 1, which shows the superimposition of the two catechol rings of AG 538 on tyrosine 1158 and 1162 in both options, straight and inverted. The best RMS is 1.9 Å of the superimposition between the two phenol-rings of IR (tyrosines 1158 and 1162) and matching atoms of AG 538.

Table 1: IGF-1R Kinase Autophosphorylation Inhibitors in a Cell-Free Assay

A.

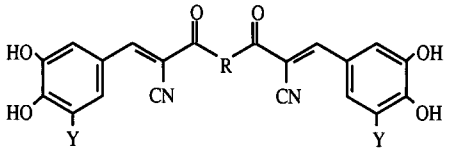

R	Y	IC_{50} (μM)	AG #
$NH(CH_2)_2NH$	OH	6.4	1717
$NH(CH_2)_4NH$	OH	2.6	575
$NH(CH_2)_5NH$	OH	13	1718
$NH(CH_2)_2NH$	H	23	548
$NH(CH_2)_3NH$	H	49	537
$NH(CH_2)_4NH$	H	4.6	550
$NH(CH_2)$-  -$(CH_2)NH$	H	4.4	590
$NH(CH_2)_5NH$	H	51	638
 $N(CH_2)_2NH$	H	3.2	591
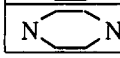 $N(CH_2)NH$	H	0.6	593

B.

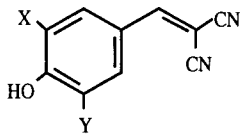

X	Y	IC_{50} (μM)	AG#
OH	I	19	974
OH	t-Bu	23	1034
OH	OH	89	82
OH	OCH_3	229	34
OH	NO_2	>250	1288
OH	H	>300	18
t-Bu	Br	98	1024
I	I	17	1049
i-Pr	i-Pr	>300	1406

C.

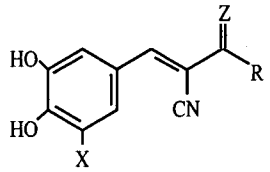

R	X	Z	IC_{50} (μM)	AG#
NH_2	H	O	>300	99
NH_2	OH	O	81.3	775
NH_2	H	S	8.1	213
NHC_6H_5	H	O	115	494
$NHCH_2C_6H_5$	H	O	138	490
$NHCH_2C_6H_5$	H	S	1.8	1007
$NHCH_2C_6H_5$	I	O	9.1	1505
$NH(CH_2)_3C_6H_5$	I	O	4.8	1387
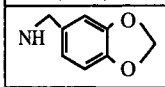	I	O	60	1668
	H	O	0.4	538
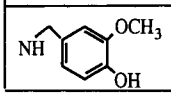	H	O	61	1661

D.

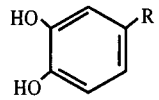

R	IC_{50} (μM)	AG#
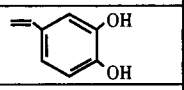	0.48	1233
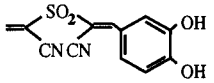	1.7	1076

The hydroxyl groups of AG 538 are in close proximity to the hydroxyl groups of the tyrosine residues that undergo autophosphorylation. This exercise shows that AG 538 can substitute for tyrosines 1158 and 1162, which occupy the auto-substrate site. This finding suggests that AG 538 is competitive with the substrate and not with ATP.

AG 538 Competes with IGF-1R Substrate and Not with ATP. Table 3 shows that the IC_{50} for the inhibition of IGF-1R autophosphorylation is independent of ATP over a wide concentration range. This finding further supports the contention that AG 538 is noncompetitive with ATP.

The use of the radioactive method (described in the Materials and Methods) allowed us to perform kinetic analysis of IGF-1R inhibition by AG 538. The analysis shows clearly that the compound is competitive with the substrate (Figure 2, Table 4).

AG 538 Inhibits Other Kinases Less Efficiently Than It Blocks IGF-1R and IR. Substrate phosphorylation by other kinases were performed in the presence of AG 538. This inhibitor was found not to inhibit PKB or Src but to inhibit the insulin receptor kinase (IR) with similar efficacy to that of the IGF-1R (Table 5). AG 538 inhibits the EGFR with

Table 2: Inhibition of pGT Phosphorylation by the IGF-1R

A.

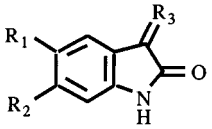

R_1	R_2	R_3	IC_{50} μM	AG #
NO_2	H		>100	217
H	H		>100	242
OH	H		>100	250
OH	OCH_3	O	>20	251
OH	OCH_3		8	252
OCH_3	OCH_3	O	>100	1693
OCH_3	OCH_3	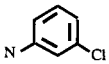	>100	1694
H	H	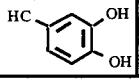	14.8	2101

B.

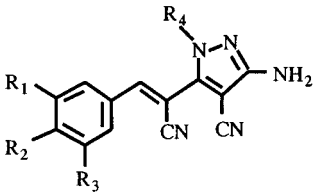

R_1	R_2	R_3	R_4	IC_{50} μM	AG #
OH	OH	H	H	5	568
OH	OH	H		4	1111
t-Bu	OH	t-Bu	H	>100	1393
i-Pr	OH	i-Pr	H	>100	1500
OCH_3	OH	I	H	>100	1501
H	NO_2	H	H	>25	1843

10-fold reduced efficacy as compared to IGF-1R (Table 5). The Src, IR, and IGF-1R inhibition assays were performed using 20 μM of ATP, and the PKB assay was performed using 10 μM ATP. The assays for Src and PKB will be described elsewhere (Karni et al., in preparation; Reuveni et al., in preparation). The assay for EGFR kinase inhibition was performed in the presence of 125 μM ATP (*34*).

Inhibition of Downstream Signaling Elements. I-OMe-AG 538 inhibits in vitro IGF-1R autophosphorylation with an $IC_{50} = 3.4 \pm 0.5$ μM and pGT phosphorylation with an $IC_{50} = 2 \pm 0.8$ μM as compared to 0.4 ± 0.2 μM and 61 ± 20 nM, respectively, for AG 538. To assay inhibition in intact cells, subconfluent cells were incubated with AG 538 (Figure 3) or I-OMe AG 538 (Figure 4) as described in the Materials and Methods. Gels were blotted and probed with anti-phosphotyrosine 4G10 and anti-IGF-1R antibodies (Figures 3A and 4A respectively), anti-phospho-Akt and anti-Akt antibodies (Figures 3B and 4B), and phospho Erk and anti-Erk2 antibodies (Figures 3C and 4C). IGF-1R autophosphorylation, Erk activation, and PKB/Akt activation were all inhibited in a dose responsive manner by AG 538 and by I-OMe AG (Figure 3 and 4).

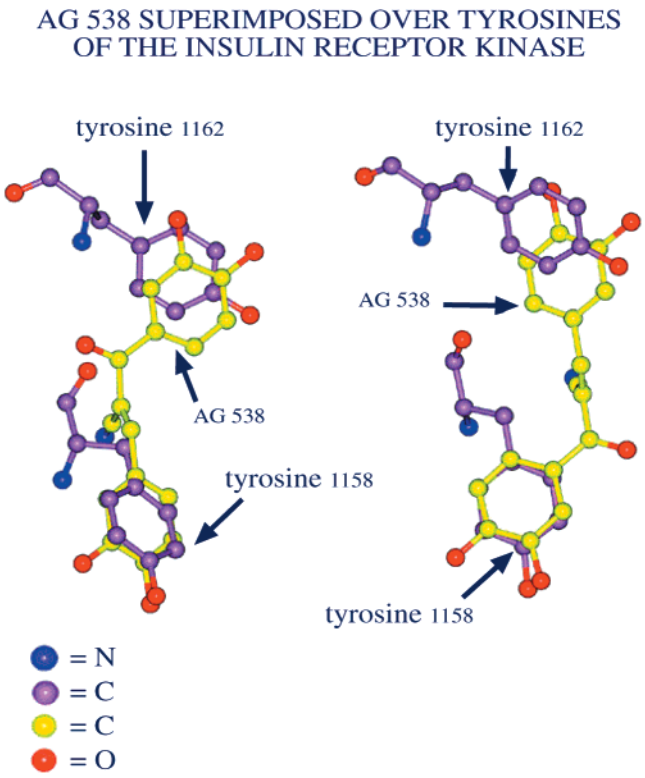

FIGURE 1: Alignment of AG 538 into the kinase site of Insulin Receptor. The two catechol rings of AG 538 (yellow) superimposed over tyrosines 1158 and 1162 of the IR kinase domain (purple). On the right the catechol closest to the carbonyl is superimposed on tyrosine 1158, the other catechol is superimposed on tyrosine 1162. The left panel shows the same superimposition with AG 538 rotated by 180°.

Table 3: Inhibition of IGF-1 Autophosphorylation by AG 538 at Different ATP Concentrations

IC_{50} of AG 538 (μM)	ATP concentration (μM)
0.29 ± 0.07	2
0.14 ± 0.05	6
0.24 ± 0.03	15
0.22 ± 0.05	30
0.24 ± 0.07	60
0.26 ± 0.03	100

DISCUSSION

In this report, we describe two nonradioactive cell-free assays for the inhibition of IGF-1R kinase. The first assay, for tyrosine autophosphorylation inhibition, is based on immunoprecipitating the receptor onto an ELISA plate. The second assay is based on tyrosine phosphorylation of a plate bound substrate, pGT. These assays are useful to screen potential IGF-1R inhibitors. We chose tyrphostins which were likely to compete with the substrate site and possibly

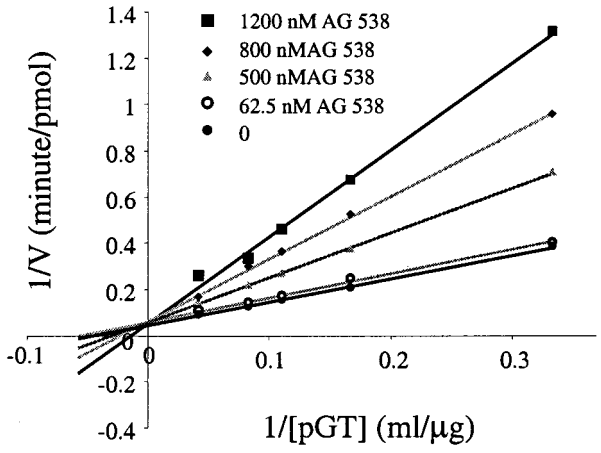

FIGURE 2: Inhibition of IGF-1R catalyzed phosphorylation of pGT. Poly-GT was phosphorylated by semipurified IGF-1R, and the activity of the IGF-1R was determined by the radioactive method described in Materials and Methods. Various concentrations of pGT and AG 538 were used in each system.

Table 4: Effect of pGT Concentration on IC50 of IGF-1R Inhibition by AG 538

pGT (μg/mL)	IC_{50} (μM)
3.7	0.130
11.1	0.214
33.3	0.460
300	0.860

Table 5: Inhibition of Various Kinases by AG 538

enzyme	substrate	IC_{50} (nM)
IGF-1R	pGT	60
IR	pGT	113
EGF−R	pGAT	370
Src	pGT	2400
PKB	RPRTSSF	76 000

compete with tyrosines 1158 and 1162 which are bound the substrate binding site of the receptor. We therefore chose tyrphostins with two aromatic rings, within the library of compounds which we possess. Structure function analysis of the compounds screened led to some lead compounds. The most potent inhibitor was identified as AG 538 (Table 1). AG 538 could indeed be minimized and "docked" to the site occupied by Y1158/Y1162 in the nonactivated IR (Figure 1).

The successful superimposition of AG 538 over the IR tyrosines 1158 and 1162 suggests that AG 538 competes with the IGF-1R tyrosines at the autophosphorylation site, thus inhibiting IGF-1R autophosphorylation. Our assumption was validated by the finding that AG 538 is noncompetitive with ATP (Table 3), and is competitive with the substrate pGT (Figure 2). The utilization of the three-dimensional structure of the homologous IR, as a basis for the search for an IGF-1R inhibitor, was expected to produce inhibitors against both IR and IGF-1R. Indeed, AG 538 (Table 5) and I-OMe AG 538 inhibit the insulin receptor with IC_{50} values similar to those of for IGF-1R kinase inhibition (data not shown). The compounds must therefore be further modified in accordance with structure function analysis to diminish or abolish IR kinase inhibition. We believe that by using the two assays, for IR and for IGF-1R substrate phosphorylation inhibition, side by side, it should be possible to make steady progress toward selective substrate-competitive inhibitors of IGF-1R kinase.

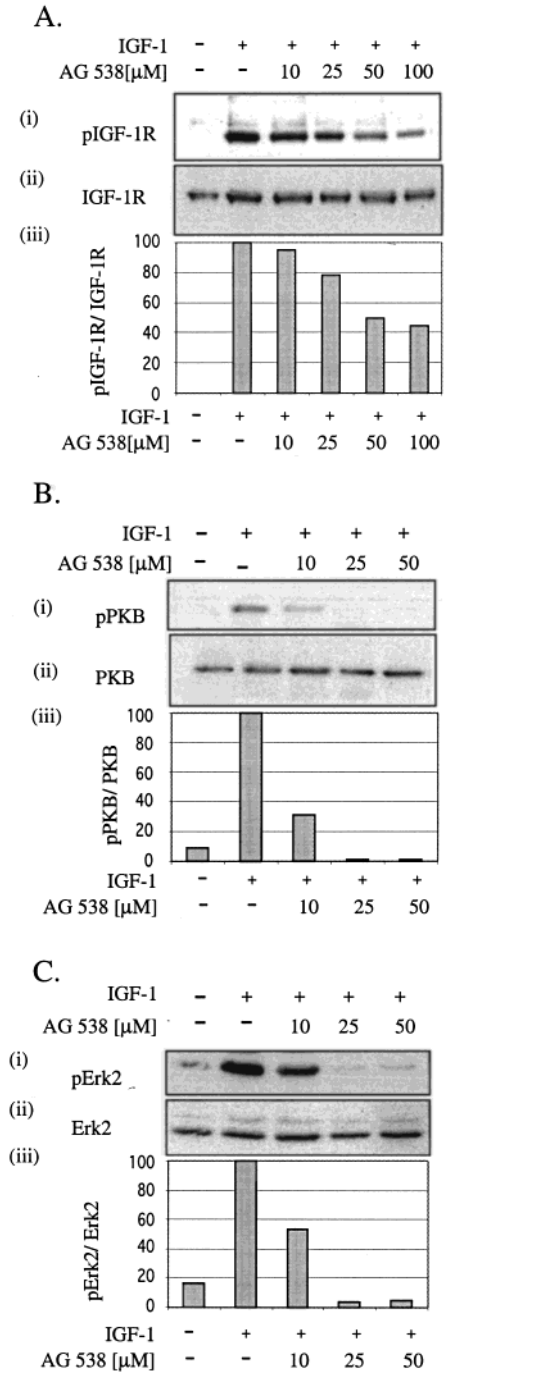

FIGURE 3: Inhibition of IGF-1R signaling by AG 538. (A) Inhibition of IGF-1R autophosphorylation by AG 538. (i) Western blot using α-phosphotyrosine 4G10 antibody. (ii) Reprobing of stripped blot with α-IGF-1Rβ antibody. (iii) The phosphorylation level of each sample [shown in panel A(i)] was normalized to the IGF-1R level shown in panel A(ii). These values are shown as percentages of the level of autophosphorylation in the absence of inhibitor (designated 100%). (B) Inhibition of PKB phosphorylation by AG 538. (i) Western blot using αphosphoserine 473 antibody. (ii) Reprobing of stripped blot with α-PKB/Akt1 antibody. (iii) Percent of maximum phosphorylation for each sample was defined in the same manner described in panel A(iii). (C) Inhibition of Erk2 phosphorylation by AG 538. (i) Western blot using anti-D-P-Erk1&2 antibody. (ii) Reprobing of stripped blot with α-Erk2 antibody. (iii) Percent of maximum phosphorylation for each sample was defined in the same manner described in panel A(iii).

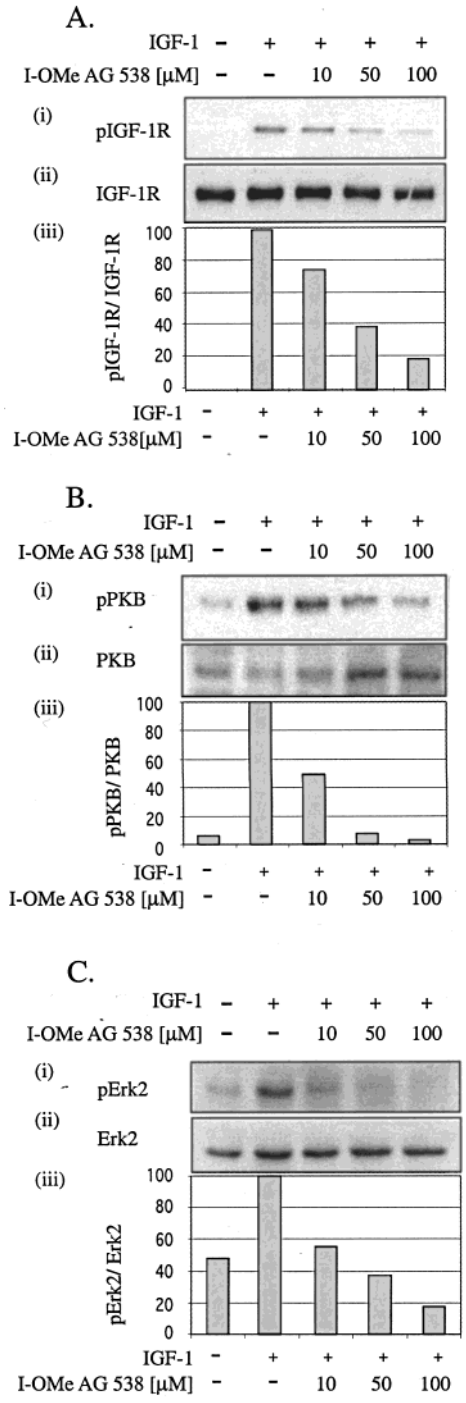

FIGURE 4: Inhibition of IGF-1R signaling by I-OMe-AG538. Experimental details as described in Figure 3.

Compounds that block enzyme function by substrate competition may have an advantage over ATP-mimicking inhibitors. First, the high intracellular concentration of ATP may reduce the efficacy of ATP mimics. Second, a substrate-competitive inhibitor is likely to be more selective than an ATP-competitive inhibitor, because there are many ATP-dependent enzymes.

Structure function relationship led us to the synthesis of a hydrophobic analogue of AG 538, that tends to oxidize less since it contains iodine and a methyl group (I-OMe AG 538) substituting partly for the hydroxyls. This compound, although possessing lower cell-free efficacy than AG 538, inhibits the IGF-1R autophosphorylation as well as IGF-1R downstream targets PKB and Erks, in a similar dose-dependent manner (Figure 4) as AG 538 (Figure 3) in cellular assays. Most probably, the enhanced hydrophobicity of I-OMe AG 538 allows it to penetrate more readily than AG 538 and inhibit the activation of intracellular targets in a similar concentration range as AG 538 does. It seems that the enhanced hydrophobicity of I-OMe-AG 538 compensates for the reduced intrinsic affinity to the receptor.

The finding that AG 538 is more potent against EGFR than Src (Table 5) may suggest that there are more similarities between the substrate binding sites between IGF-1R/IR and EGFR than between IGF-1R/IR and Src. This point requires further investigation.

We are presently engaged in designing combinatorial libraries based on AG 538 and I-OMe AG 538 in order to obtain more potent substrate competitive cell permeable inhibitors of IGF-1R.

ACKNOWLEDGMENT

We would like to thank Michael Engel for helping with the analysis of the kinetics. We would like to thank Ella Sklan and Tamar Geiger for the results of Src and PKB kinase inhibition. This study was partially supported by a grant from the Deutsches Krebsforschungszentrum.

REFERENCES

1. Hernandez-Sanchez, C., Blakesley, V., Kalebic, T., Helman, L., and LeRoith, D. (1995) *J. Biol. Chem. 270*, 29176−81.
2. LeRoith, D., Sampson, P. C., and Roberts, C. T., Jr. (1994) *Horm. Res. 41 Suppl. 2*, 74−8, see discussion 79.
3. Parrizas, M., Saltiel, A. R., and LeRoith, D. (1997) *J. Biol. Chem. 272*, 154−61.
4. Rubin, R., and Baserga, R. (1995) *Lab. Invest. 73*, 311−31.
5. Benito, M., Valverde, A. M., and Lorenzo, M. (1996) *Int. J. Biochem., Cell Biol. 28*, 499−510.
6. Reeve, J. G., Brinkman, A., Hughes, S., Mitchell, J., Schwander, J., and Bleehen, N. M. (1992) *J. Natl. Cancer Inst. 84*, 628−34.
7. Lahm, H., Suardet, L., Laurent, P. L., Fischer, J. R., Ceyhan, A., Givel, J. C., and Odartchenko, N. (1992) *Br. J. Cancer 65*, 341−6.
8. Antoniades, H. N., Galanopoulos, T., Neville-Golden, J., and Maxwell, M. (1992) *Int. J. Cancer 50*, 215−22.
9. Steller, M. A., Delgado, C. H., Bartels, C. J., Woodworth, C. D., and Zou, Z. (1996) *Cancer Res. 56*, 1761−5.
10. Werner, H., Re, G. G., Drummond, I. A., Sukhatme, V. P., Rauscher, F. J. d., Sens, D. A., Garvin, A. J., LeRoith, D., and Roberts, C. T., Jr. (1993) *Proc. Natl. Acad. Sci. U.S.A. 90*, 5828−32.
11. Prager, D., Li, H. L., Asa, S., and Melmed, S. (1994) *Proc. Natl. Acad. Sci. U.S.A. 91*, 2181−5.
12. Arteaga, C. L., and Osborne, C. K. (1989) *Cancer Res. 49*, 6237−41.
13. Gansler, T., Furlanetto, R., Gramling, T. S., Robinson, K. A., Blocker, N., Buse, M. G., Sens, D. A., and Garvin, A. J. (1989) *Am. J. Pathol. 135*, 961−6.
14. Neuenschwander, S., Roberts, C. T., Jr., and LeRoith, D. (1995) *Endocrinology 136*, 4298−303.
15. Shapiro, D. N., Jones, B. G., Shapiro, L. H., Dias, P., and Houghton, P. J. (1994) *J. Clin. Invest. 94*, 1235−42.
16. Kaleko, M., Rutter, W. J., and Miller, A. D. (1990) *Mol. Cell Biol. 10*, 464−73.
17. Sell, C., Baserga, R., and Rubin, R. (1995) *Cancer Res. 55*, 303−6.
18. Dunn, S. E., Hardman, R. A., Kari, F. W., and Barrett, J. C. (1997) *Cancer Res. 57*, 2687−93.
19. Kandel, E. S., and Hay, N. (1999) *Exp. Cell Res. 253*, 210−29.

20. O'Connor, R., Kauffmann-Zeh, A., Liu, Y., Lehar, S., Evan, G. I., Baserga, R., and Blattler, W. A. (1997) *Mol. Cell Biol. 17*, 427−35.
21. Levitzki, A. (1996) *Curr. Opin. Cell Biol. 8*, 239−44.
22. Hubbard, S. R., Wei, L., Ellis, L., and Hendrickson, W. A. (1994) *Nature 372*, 746−54.
23. Hubbard, S. R. (1997) *EMBO J. 16*, 5572−81.
24. Parrizas, M., Gazit, A., Levitzki, A., Wertheimer, E., and LeRoith, D. (1997) *Endocrinology 138*, 1427−33.
25. Gazit, A., Osherov, N., Posner, I., Yaish, P., Poradosu, E., Gilon, C., and Levitzki, A. (1991) *J. Med. Chem. 34*, 1896−907.
26. Gazit, A., Yaish, P., Gilon, C., and Levitzki, A. (1989) *J. Med. Chem. 32*, 2344−52.
27. Gazit, A., Osherov, N., Posner, I., Bar-Sinai, A., Gilon, C., and Levitzki, A. (1993) *J. Med. Chem. 36*, 3556−64.
28. Gazit, A., Osherov, N., Gilon, C., and Levitzki, A. (1996) *J. Med. Chem. 39*, 4905−11.
29. Gazit, A., App, H., McMahon, G., Chen, J., Levitzki, A., and Bohmer, F. D. (1996) *J. Med. Chem. 39*, 2170−7.
30. Gazit, A., Chen, J., App, H., McMahon, G., Hirth, P., Chen, I., and Levitzki, A. (1996) *Bioorg. Med. Chem. 4*, 1203−7.
31. D'Ambrosio, C., Valentinis, B., Prisco, M., Reiss, K., Rubini, M., and Baserga, R. (1997) *Cancer Res. 57*, 3264−71.
32. Carter, W. G., Sullivan, A. C., Asamoah, K. A., and Sale, G. J. (1996) *Biochemistry 35*, 14340−51.
33. Posner, I., Engel, M., Gazit, A., and Levitzki, A. (1994) *Mol. Pharmacol. 45*, 673−83.
34. Yaish, P., Gazit, A., Gilon, C., and Levitzki, A. (1988) *Science 242*, 933−5.

BI001516Y